Inspiral-merger-ringdown waveforms for black-hole binaries with non-precessing spins

P. Ajith,[1,2,3] M. Hannam,[4,5] S. Husa,[6] Y. Chen,[2] B. Brügmann,[7] N. Dorband,[8]
D. Müller,[7] F. Ohme,[8] D. Pollney,[8] C. Reisswig,[8] L. Santamaría,[8] and J. Seiler[8]

[1]*LIGO Laboratory, California Institute of Technology, Pasadena, CA 91125, USA*
[2]*Theoretical Astrophysics, California Institute of Technology, Pasadena, CA 91125, USA*
[3]*Max-Planck-Institut für Gravitationsphysik (Albert-Einstein-Institut), Callinstr. 38, 30167 Hannover, Germany*
[4]*Physics Department, University College Cork, Cork, Ireland*
[5]*Gravitational Physics, Faculty of Physics, University of Vienna, Boltzmanngasse 5, A-1090 Vienna, Austria*
[6]*Departament de Física, Universitat de les Illes Balears, Crta. Valldemossa km 7.5, E-07122 Palma, Spain*
[7]*Theoretisch-Physikalisches Institut, Friedrich Schiller Universität Jena, Max-Wien-Platz 1, 07743 Jena, Germany*
[8]*Max-Planck-Institut für Gravitationsphysik (Albert-Einstein-Institut), Am Mühlenberg 1, 14476 Golm, Germany*

We present the first analytical inspiral-merger-ringdown gravitational waveforms from binary black holes (BBHs) with non-precessing spins that is based on a description of the late-inspiral, merger and ringdown in full general relativity (GR). By matching a post-Newtonian description of the inspiral to a set of numerical calculations performed in full GR, we obtain a waveform family with a conveniently small number of physical parameters. The physical content of these waveforms includes the "orbital hang-up" effect, and "spin flips". These waveforms will allow us to detect a larger parameter space of BBH coalescence (including a considerable fraction of precessing binaries in the comparable-mass regime), to explore various scientific questions related to gravitational-wave astronomy, and could significantly improve the expected detection rates.

Introduction.— Coalescing black-hole (BH) binaries are among the most promising candidate sources for the first direct detection of gravitational waves (GWs). Such observations will lead to precision tests of the strong-field predictions of general relativity as well as provide a wealth of information relevant to fundamental physics, astrophysics, and cosmology. Computation of the expected waveforms from such sources is a key goal in current research in gravitation.

While the *inspiral* and *ring-down* stages of the BH coalescence are well-modeled by perturbative techniques, an accurate description of the *merger* requires numerical solutions of Einstein's equations. Although performing numerical simulations densely sampling the entire parameter space of BH coalescence is computationally prohibitive, waveform templates modeling all the three stages can now be constructed by combining analytical- and numerical-relativity results, dramatically improving the sensitivity of searches for GWs from BH binaries, and the accuracy of estimating the source parameters [1–4]. To date, inspiral-merger-ringdown (IMR) templates have been computed only for nonspinning BH binaries [1, 3–6], which are employed in GW searches, and in a number of astrophysical studies. However, nonspinning BHs are expected to be astrophysically rare, and most BHs in nature may be highly spinning [7, 8]. This necessitates the inclusion of spinning-binary waveforms in GW searches. But, spin adds six parameters (three components for each BH), and each additional parameter in a search template bank leads to a higher signal-to-noise-ratio (SNR) threshold for a confident detection [9]. Also, this requires sufficiently accurate numerical simulations across this large parameter space, which are not yet available. Moreover, implementing a search covering the full spin parameter space has proven to be difficult.

In this letter, we present an IMR waveform family modeling the dominant harmonic of binaries with non-precessing spins, i.e., spins (anti-)aligned with the orbital angular momentum. Aligned-spin binaries are an astrophysically interesting population as such systems are expected from isolated binary evolution and in gas-rich galactic mergers [10, 11]. Such systems also exhibit interesting strong-gravity effects like the "orbital hang-up" [12] and "spin flips" [13]. We make use of the degeneracies in the physical parameters to parametrize our waveform family by only the total mass $M \equiv m_1 + m_2$ of the binary, the symmetric mass ratio $\eta \equiv m_1 m_2/M^2$, and a *single* spin parameter $\chi \equiv (1+\delta)\,\chi_1/2 + (1-\delta)\,\chi_2/2$, where $\delta \equiv (m_1 - m_2)/M$ and $\chi_i \equiv S_i/m_i^2$, S_i being the spin angular momentum of the ith BH. The last feature is motivated by the observation (see e.g., [14]) that the leading spin-orbit-coupling term in post-Newtonian (PN) waveforms is dominated by this parameter. We also show that this waveform family is able to capture a significant fraction of precessing binaries in the comparable-mass regime, the reason being that the phase evolution is primarily governed by the spin-orbit coupling, which is determined by the component of the spins along the angular momentum. This provides an efficient and feasible way of searching for precessing binaries in the comparable-mass regime.

Numerical simulations.— Binary BH (BBH) waveforms covering at least eight wave cycles before merger were produced by solving the full Einstein equations numerically, as written in the "moving-puncture" 3+1 formulation [15, 16]. The numerical solutions were calculated with the `BAM` [17, 18], `CCATIE` [19] and `LLAMA` [20] codes. Initial momenta were chosen to give low-eccentricity inspiral, using either an extension of the method described in [21], or the quasicircular formula used in [22]. GWs were extracted at $R_{ex} = 90M$ with `BAM`, $R_{ex} = 160M$ with `CCATIE` and at future null infinity with `LLAMA`, using the procedures discussed in [17, 19, 23]. In all simulations the GW amplitude is accurate to within *at least* 10% and the phase to within *at least* 1 radian over the duration of the simulation. Most of the waveforms employed in the construction of the analytical templates are significantly longer (12–22 cycles) and more accurate [24].

Seven sets of simulations were used in this paper: (1) Equal-mass binaries with equal, non-precessing spins $\chi_i = \pm\{0.25, 0.5, 0.75, 0.85\}$, described in [24, 25]. (2) Unequal-mass, non-precessing spin binaries with $q \equiv m_1/m_2 =$

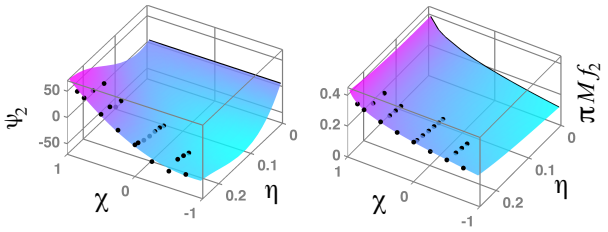

FIG. 1: Phenomenological parameters ψ_2 and f_2 computed from *equal-spin* hybrid waveforms (dots), and analytical fits given by Eq. (2) (surfaces). Test-mass limit is indicated by black traces. η is the symmetric mass ratio, χ the spin parameter, and M the total mass.

$\{2,2.5,3\}$ and $\chi_i = \{\pm 0.5, 0.75\}$. (3) Nonspinning binaries with $q = \{1,1.5,2,2.5,3,3.5,4\}$. (4) Unequal-mass, unequal-spin binaries with $q = \{2,3\}$ and $(\chi_1,\chi_2) = (-0.75,0.75)$. (5) Equal-mass, unequal-spin binaries with $\chi_i = \pm\{0.2,0.3,0.4,0.6\}$. (6) Equal-mass, precessing binaries with spin vectors $(0.42,0,0.42),(0,0,0)$ and $(0.15,0,0),(0,0,0)$. (7) Precessing binary with $q = 3$ and spins $(0.75,0,0),(0,0,0)$. The simulation sets (1)–(4) and (7) were performed with the `BAM` code, set (5) with the `CCATIE` code, and set (6) with the `LLAMA` code. The analytical waveform family is constructed *only* employing the equal-spin simulation sets (1)–(3), while sets (4)–(7) were used to test the efficacy of the template family to model the expected signals from more general spin/mass configurations. Two additional waveforms were used to test the template family: the equal-mass, non-spinning simulation performed by the Caltech-Cornell group [26], and the $q = 1.25$ precessing binary simulation with spins $(-0.09,0.48,0.35),(-0.2,-0.14,0.32)$ by the RIT group [27].

Constructing hybrid waveforms.— Following [1, 5], we produce a set of "hybrid waveforms" by matching PN and numerical-relativity (NR) waveforms in an overlapping time interval $[t_1,t_2]$. These hybrids are assumed to be the target signals that we want to detect. For the PN inspiral waveforms we choose the "TaylorT1" waveforms at 3.5PN [28] phase accuracy, considering spin terms up to 2.5PN [29, 30]. This is motivated by PN-NR comparisons of equal-mass spinning binaries, in which the accuracy of the TaylorT1 approximant was found to be the most robust [24, 25]. We include the 3PN amplitude corrections to the dominant quadrupole mode [31] and the 2PN spin-dependent corrections [14], which greatly improved the agreement between PN and NR waveforms. For precessing waveforms, the spin and angular momenta are evolved according to [30, 32].

If $\mathrm{h}(t) = h_+(t) - \mathrm{i}h_\times(t)$ denotes the time-domain waveform from a binary, we match the PN and NR waveforms by doing a least-square fit over time- and phase shifts between the waveforms, and a scale factor a that reduces the PN-NR amplitude difference. The NR waveforms are combined with the "best-matched" PN waveforms in the following way: $\mathrm{h}^{\rm hyb}(t) \equiv a\tau(t)\,\mathrm{h}^{\rm NR}(t) + (1-\tau(t))\,\mathrm{h}^{\rm PN}(t)$, where τ ranges linearly from zero to one for $t \in [t_1,t_2]$.

Waveform templates for non-precessing binaries.— The analytical waveforms that we construct can be written in the Fourier domain as $h(f) \equiv A(f)\,e^{-\mathrm{i}\Psi(f)}$, where

$$A(f) \equiv \mathscr{C} f_1^{-7/6} \begin{cases} f'^{-7/6}\,(1+\sum_{i=2}^{3}\alpha_i\,v^i) & \text{if } f < f_1 \\ w_m\,f'^{-2/3}\,(1+\sum_{i=1}^{2}\varepsilon_i\,v^i) & \text{if } f_1 \le f < f_2 \\ w_r\,\mathscr{L}(f,f_2,\sigma) & \text{if } f_2 \le f < f_3, \end{cases}$$

$$\Psi(f) \equiv 2\pi f t_0 + \varphi_0 + \frac{3}{128\eta v^5}\Big(1+\sum_{k=2}^{7} v^k\,\psi_k\Big). \qquad (1)$$

In the above expressions, $f' \equiv f/f_1$, $v \equiv (\pi M f)^{1/3}$, $\varepsilon_1 = 1.4547\,\chi - 1.8897$, $\varepsilon_2 = -1.8153\,\chi + 1.6557$ (estimated from hybrid waveforms), $\mathscr{C}$ is a numerical constant whose value depends on the sky-location, orientation and the masses, $\alpha_2 = -323/224 + 451\,\eta/168$ and $\alpha_3 = (27/8 - 11\,\eta/6)\chi$ are the PN corrections to the Fourier domain amplitude of the ($\ell = 2, m = \pm 2$ mode) PN waveform [14], t_0 is the time of arrival of the signal at the detector and φ_0 the corresponding phase, $\mathscr{L}(f,f_2,\sigma)$ a Lorentzian function with width σ centered around the frequency f_2, w_m and w_r are normalization constants chosen so as to make $A(f)$ continuous across the "transition" frequencies f_2 and f_1, and f_3 is a convenient cut-off frequency such that the power of the signal above this frequency is negligible. The phenomenological parameters ψ_k and $\mu_k \equiv \{f_1, f_2, \sigma, f_3\}$ are written in terms of the physical parameters of the binary as:

$$\psi_k = \sum_{i=1}^{3}\sum_{j=0}^{N} x_k^{(ij)}\,\eta^i\chi^j + \psi_k^0, \quad \mu_k = \sum_{i=1}^{3}\sum_{j=0}^{N} \frac{y_k^{(ij)}\,\eta^i\chi^j + \mu_k^0}{\pi M}, \qquad (2)$$

where $N \equiv \min(3-i,2)$ while $x_k^{(ij)}$ and $y_k^{(ij)}$ are tabulated in Table I. Figure 1 plots an example of this map from the phenomenological- to physical- parameter space.

We match these waveforms to 2PN accurate adiabatic inspiral waveforms in the test-mass limit. In the $\eta \to 0$ limit, the phenomenological parameters reduce to the following:

$$f_1 \to f^0_{\rm LSO}, \;\; f_2 \to f^0_{\rm QNM}, \;\; \sigma \to f^0_{\rm QNM}/Q^0, \;\; \psi_k \to \psi^0_k, \qquad (3)$$

where $f^0_{\rm LSO}$ and $f^0_{\rm QNM}$ are the frequencies of the last stable orbit [33] and the dominant quasi-normal mode, and Q^0 is the ring-down quality factor [34] of a Kerr BH with mass M and spin χ, while ψ^0_k are the (2PN) Fourier domain phasing coefficients of a test-particle inspiralling into the Kerr BH, computed using the stationary-phase approximation [14].

The test-particle-limit waveforms suffer from two limitations: 1) we assume that the evolution of the GW phase at the merger and ringdown stages is a continuation of the adiabatic inspiral phase, and 2) in the absence of a reliable plunge model, we approximate the amplitude of the plunge with $f'^{-2/3}\,(1+\sum_{i=1}^{2}\varepsilon_i\,v^i)$. Nevertheless, in the test-mass limit, it is expected that the signal will be dominated by the long inspiral stage (followed by a quick plunge and ringdown), and the inspiral is guaranteed to be well-modelled by our waveforms. More importantly, the imposition of the appropriate test-mass limit in our fitting procedure ensures that the waveforms are well behaved even outside the parameter range where current NR data are available. Because of this, and the inclusion of

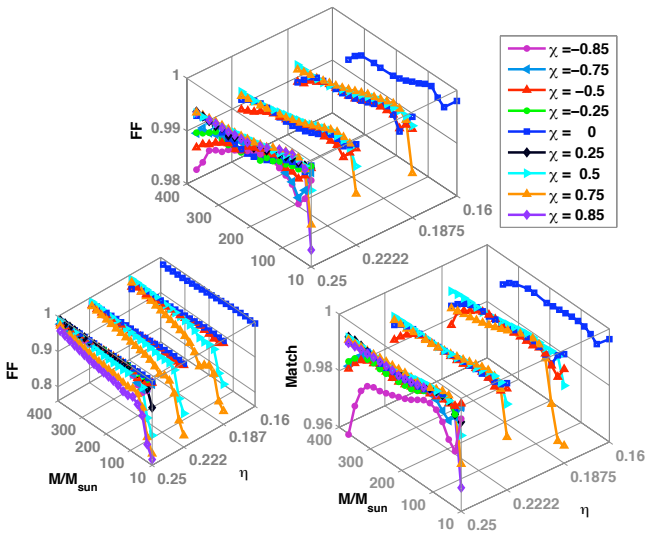

FIG. 2: *Top and right plots*: Match and FF of our analytical IMR templates with equal-spin hybrid waveforms constructed from simulation sets (1)–(3). *Bottom left*: FF of *non-spinning* IMR templates proposed in [1, 6] with the equal-spin hybrid waveforms. A comparison with the other plots demonstrates the effect of neglecting spins.

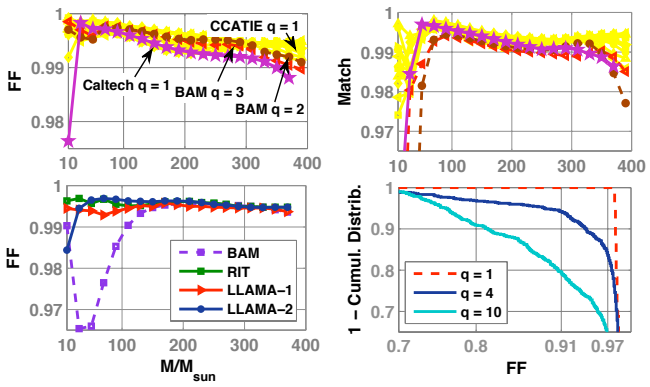

FIG. 3: *Top panel:* Match and FF of the our templates with *unequal-spin* hybrid waveforms constructed from simulation sets (4) and (5), and the Caltech-Cornell non-spinning simulation. *Bottom left:* FF with *precessing* hybrids constructed from sets (6) and (7), and the RIT simulation. *Bottom right:* Fraction of generic precessing PN waveforms ($M = 20M_\odot$) producing fitting factor FF with the templates proposed in this paper — 100% (85%) 65% of the binaries with $q = 1(4)10$ produce FF > 0.965.

the PN amplitude corrections, these waveforms are expected to be closer to the actual signals than the templates proposed in [1, 6] in the non-spinning limit. However, since the parameter space covered by the NR simulations is limited, we recommend that these waveforms be used only in the regime $q \lesssim 10$ and $-0.85 \lesssim \chi \lesssim 0.85$. Also, these are meant to model only the late-inspiral, merger and ring down ($M f_{\rm GW} > 10^{-3}$), i.e., signals from binaries in the mass-range where merger-ringdown also contribute to the SNR, apart from inspiral.

We have examined the "faithfulness" [35] of the new templates in reproducing the hybrid waveforms by computing the *match* (noise-weighted inner product) with the hybrids. Loss of the SNR due to the "mismatch" between the template and the true signal is determined by the match maximized over the whole template bank – called *fitting factor* (FF). The standard criteria for templates used in searches is that FF > 0.965, which corresponds to a loss of no more than 10% of signals.

Match and FF of the analytical waveforms with the equal- (unequal-) spin hybrid waveforms are plotted in Fig. 2 (Fig. 3), using the Initial LIGO design noise spectrum [36]. Note that the analytical waveform family is constructed employing *only* the equal-spin hybrid waveforms (Fig. 2). The PN–NR matching region used to construct the unequal-spin hybrids (Fig. 3) are also different from that used for equal-spin hybrids. These figures demonstrate the efficacy of the analytical templates in reproducing the target waveforms – templates are "faithful" (match > 0.965) *either* when the masses *or* the spins are equal, while they are *always* "effectual" [35] in detection (FF > 0.965) [37]. In contrast, the bottom left plot of Fig. 2 shows the FF of the non-spinning IMR template family proposed in [1, 6] with the equal-spin hybrid waveforms. FFs as low as 0.8 suggest that up to 50% binaries may go undetected if nonspinning IMR templates are employed to search for binaries with high (aligned) spins.

Bottom left plot of Fig. 3 shows the FF and match of the template family with four *precessing* hybrid waveforms. The high FFs are indicative of the effectualness of the templates in detecting precessing binaries. Since presently not enough NR simulations are available to make a quantitative statement, and since we expect the effect of precession will be predominant in the case of lower mass binaries (when large number of cycles are present in the detectors band), we might be able to acquire some useful indication by studying precessing PN waveforms. We have performed a Monte-Carlo simulation where we generate generic precessing "restricted" 3.5PN waveforms (with 2.5PN spin corrections) with $M = 20M_\odot$, $q = \{1, 4, 10\}$ and spins uniformly distributed in a sphere of radius 0.98, and compute the FF with the templates proposed in this paper. Inclination of the binary's plane with the line of sight from the observer is also randomly selected from $[0, \frac{\pi}{2}]$. Bottom right plot of Fig. 3 shows the cumulative distribution of the FF, strongly indicating the effectualness of the templates in detecting precessing binaries in the comparable-mass regime. Almost all binaries producing FF < 0.965 have (the astrophysically less likely [10]) tilt angles $> \frac{\pi}{2}$ for the massive BH, and undergo flipping of the orbital plane.

Distance to optimally oriented BBHs producing optimal SNR of 8 at Initial LIGO noise spectrum is shown in Fig. 4, which demonstrates the dramatic effect of spin for detection of high-mass binaries; if most BBHs are highly spinning, then LIGO will be able to detect BH coalescences up to 1Gpc, thus increasing the event rates as much as five times compared to predictions based on models of nonspinning binaries. For Advanced LIGO, the distance reach is as high as 20 Gpc.

Conclusions.— We combine state-of-the-art results from analytical- and numerical relativity to construct for the first time a family of analytical IMR waveforms for BBHs with non-precessing spins from "first principles". These waveforms are also able to detect a significant fraction of the precessing binaries in the comparable-mass regime, and we show that for the purposes of GW detection it is sufficient to rep-

	Test-mass limit (ψ_k^0)	$x^{(10)}$	$x^{(11)}$	$x^{(12)}$	$x^{(20)}$	$x^{(21)}$	$x^{(30)}$
ψ_2	$3715/756$	-920.9	492.1	135	6742	-1053	-1.34×10^4
ψ_3	$-16\pi+113\chi/3$	1.702×10^4	-9566	-2182	-1.214×10^5	2.075×10^4	2.386×10^5
ψ_4	$15293365/508032-405\chi^2/8$	-1.254×10^5	7.507×10^4	1.338×10^4	8.735×10^5	-1.657×10^5	-1.694×10^6
ψ_6	0	-8.898×10^5	6.31×10^5	5.068×10^4	5.981×10^6	-1.415×10^6	-1.128×10^7
ψ_7	0	8.696×10^5	-6.71×10^5	-3.008×10^4	-5.838×10^6	1.514×10^6	1.089×10^7
	Test-mass limit (μ_k^0)	$y^{(10)}$	$y^{(11)}$	$y^{(12)}$	$y^{(20)}$	$y^{(21)}$	$y^{(30)}$
f_1	$1-4.455(1-\chi)^{0.217}+3.521(1-\chi)^{0.26}$	0.6437	0.827	-0.2706	-0.05822	-3.935	-7.092
f_2	$[1-0.63(1-\chi)^{0.3}]/2$	0.1469	-0.1228	-0.02609	-0.0249	0.1701	2.325
σ	$[1-0.63(1-\chi)^{0.3}](1-\chi)^{0.45}/4$	-0.4098	-0.03523	0.1008	1.829	-0.02017	-2.87
f_3	$0.3236+0.04894\chi+0.01346\chi^2$	-0.1331	-0.08172	0.1451	-0.2714	0.1279	4.922

TABLE I: Phenomenological parameters describing the analytical waveforms (see Eq. (2)). In test-mass limit, they reduce to the appropriate quantities given by perturbative calculations [14, 33, 34]. The test-mass limit of f_1 is a fit to the frequency at the last stable orbit given in [33].

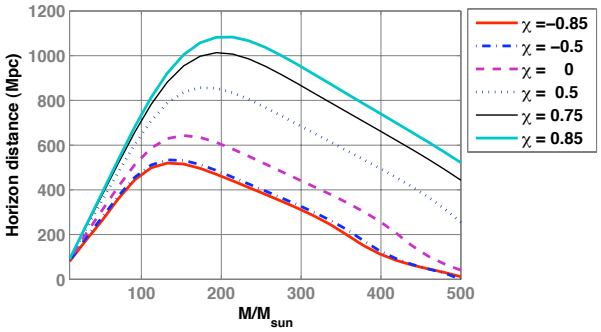

FIG. 4: Distance to optimally-located and oriented- equal-mass binaries with (equal) spin χ producing optimal SNR 8 in Initial LIGO.

resent the spins by a *single* parameter. This will considerably simplify the use of our waveforms in GW searches in the near future, and will accelerate the incorporation of NR results into the current effort for the first detection of GWs. There are many other immediate applications of our waveforms: injections into detector data will help to put more realistic upper limits on the rate of BBH coalescences, and to compare the different algorithms employed in the search for BBHs, while employing these in population-synthesis studies will provide more accurate coalescence rates observable by the current and future detectors. Our method can readily be generalized to incorporate non-quadrupole harmonics, larger portions of the BBH parameter space and further information from analytical approximation methods or numerical simulations.

SH was supported in part as a VESF fellow of EGO, by DAAD grant D/07/13385 and grant FPA-2007-60220 from the Spanish Ministerio de Educación y Ciencia. MH was supported by SFI grant 07/RFP/PHYF148 and an FWF Lise Meitner fellowship (M1178-N16). PA and YC were supported in part by NSF grants PHY-0653653, PHY-0601459, PHY-0956189 and the David and Barbara Groce Fund at Caltech. BB is supported in part by DFG grant SFB/Transregio 7 "Gravitational Wave Astronomy", BB and DM by the DLR, and LS by DAAD grant A/06/12630. We thank the Albert Einstein Institute, University of Jena, LRZ, ICHEC, CESGA and BSC-CNS for providing computational resources, and K. G. Arun, B. Sathyaprakash, G. Faye and R. O'Shaughnessy for useful discussions / comments.

[1] P. Ajith et al., Phys. Rev. D **77**, 104017 (2008).
[2] P. Ajith and S. Bose, Phys. Rev. D **79**, 084032 (2009).
[3] A. Buonanno et al., Phys. Rev. D **76**, 104049 (2007).
[4] T. Damour and A. Nagar, Phys. Rev. D **79**, 081503 (2009).
[5] P. Ajith et al., Class. Quant. Grav. **24**, S689 (2007).
[6] P. Ajith, Class. Quant. Grav. **25**, 114033 (2008).
[7] M. Volonteri et al., Astrophys. J. **620**, 69 (2005).
[8] C. F. Gammie et al., Astrophys. J. **602**, 312 (2004).
[9] C. Van Den Broeck et al., Phys. Rev. D **80**, 024009 (2009).
[10] V. Kalogera, Pramana **63**, 673 (2004).
[11] T. Bogdanović et al., Astrophys. J. **661**, L147 (2007).
[12] M. Campanelli et al., Phys. Rev. D **74**, 041501(R) (2006).
[13] A. Buonanno et al., Phys. Rev. D **77**, 026004 (2008).
[14] K. G. Arun et al., Phys. Rev. D **79**, 104023 (2009).
[15] M. Campanelli et al., Phys. Rev. Lett. **96**, 111101 (2006).
[16] J. G. Baker et al., Phys. Rev. Lett. **96**, 111102 (2006).
[17] B. Brügmann et al., Phys. Rev. D **77**, 024027 (2008).
[18] S. Husa et al., Class. Quant. Grav. **25**, 105006 (2008).
[19] D. Pollney et al., Phys. Rev. D **76**, 124002 (2007).
[20] D. Pollney et al. (2009), arXiv:0910.3803.
[21] S. Husa et al., Phys. Rev. D **77**, 044037 (2008).
[22] B. Brügmann et al., Phys. Rev. D **77**, 124047 (2008).
[23] C. Reisswig et al., Phys. Rev. Lett. **103**, 221101 (2009).
[24] M. Hannam et al. (2010), arXiv:1007.4789.
[25] M. Hannam et al., Phys. Rev. D **78**, 104007 (2008).
[26] M. A. Scheel et al., Phys. Rev. D **79**, 024003 (2009).
[27] M. Campanelli et al., Phys. Rev. D **79**, 084010 (2009).
[28] L. Blanchet et al., Phys. Rev. Lett. **93**, 091101 (2004).
[29] L. Blanchet et al., Phys. Rev. D **74**, 104034 (2006).
[30] E. Racine et al., Phys. Rev. D **80**, 044010 (2009).
[31] L. Blanchet et al., Class. Quant. Grav. **25**, 165003 (2008).
[32] A. Buonanno et al., Phys. Rev. D **67**, 104025 (2003).
[33] J. M. Bardeen et al., Astrophys. J. **178**, 347 (1972).
[34] F. Echeverria, Phys. Rev. D **40**, 3194 (1989).
[35] T. Damour et al., Phys. Rev. D **57**, 885 (1998).
[36] http://www.ligo.caltech.edu/∼jzweizig/distribution/LSC_Data.
[37] Analysis with hybrid waveforms constructed using "TaylorT4" PN waveforms also produced high FFs.